SMiRT-12 / K. Kussmaul (Editor)

G05/6

SURFACE CRACKS IN TOROIDAL SHELLS

F. Erdogan[1] and P.F. Joseph[2]

[1]Lehigh University, Bethlehem, PA, USA
[2]Clemson University, Clemson, SC, USA

ABSTRACT

Toroidal shells containing a surface crack and subjected to various symmetric and antisymmetric loading conditions are considered. Stress intensity factors are given for spherical caps and pipe elbows for different crack locations.

1. INTRODUCTION

For the purpose of analyzing stresses and performing service life estimates, many of the load bearing critical components such as domes, elbows and nozzles in nuclear power plants may be considered as *toroidal shells* in that at a certain location they generally have two distinct principal curvatures and their thickness is small relative to the radii of curvature. The stresses are usually induced by pressure, temperature changes, misalignments, and possibly by small amplitude vibrations. Because of the complexity of the component geometry and loading conditions, in most cases locally the shell is subjected to bending and transverse shear as well as membrane stresses. Thus, for an arbitrary crack orientation the problem is always a mixed mode problem. However, if the crack is located in a principal plane of curvature, the mode I solution due to membrane and bending loads can be separated, whereas modes II and III stress states due to in plane and transverse shear and twisting moment are always coupled.

In this study, after a very brief description of the method used to solve the general problem, the results for surface cracks in toroidal shells will be presented. The review of the field, with comprehensive references, the details of the analysis and extensive results for surface cracks in plates and in cylindrical shells may be found in [1]-[4].

2. FORMULATION OF THE PROBLEM

Consider the part-through crack problem described in Fig. 1. It is assumed that the surface crack is symmetrically located either inside or outside the shell in a plane of principal curvature in any one of the four positions A-D shown in the figure. Referring to Fig. 1 for notation, the mixed boundary value problem is formulated in terms of the following complementary *displacements* and *stress resultants*:

$$v(x_1,x_2) = (v_i) = (u_1,\beta_1,u_3,u_2,\beta_2)\ ,\ f(x_1,x_2) = (f_i) = (N_{11},M_{11},V_1,N_{12},M_{12})\ , \tag{1}$$

where u_i and β_j are respectively the midsurface displacements and rotations. By using the *line spring model* to represent the net ligament under the crack (Fig. 1), and referring, for example, to [4] for details, the integral equations of the problem may be expressed as

$$\frac{1}{\pi}\int_{-a}^{a}\frac{g_i(t)}{t-x_2}dt + \int_{-a}^{a}\sum_{1}^{5}K_{ij}(x_2,t)g_j(t)dt + \sum_{1}^{5}b_{ij}\int_{-a}^{x_2}g_j(t)dt = \frac{\sigma_i^o(x_2)}{B_i}\ ,\ i=1,...,5,\ |x_2|<a\ , \tag{2}$$

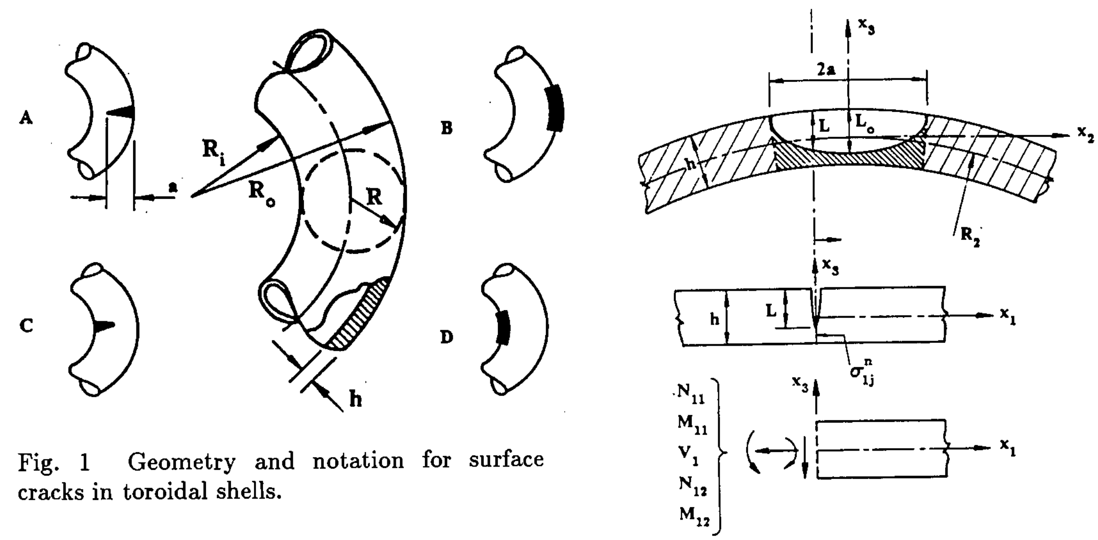

Fig. 1 Geometry and notation for surface cracks in toroidal shells.

where K_{ij} are known functions representing the shell geometry, b_{ij} are known constants coming from the line spring model, B_i are various stiffness parameters associated with (v_i,f_i), $\sigma_i{}^o$ are known functions related to the applied stress resultants by

$$(\sigma_i{}^o) = (\frac{N_{11}{}^o}{h}, \frac{6M_{11}{}^o}{h^2}, \frac{3V_1{}^o}{2h}, \frac{N_{12}{}^o}{h}, \frac{6M_{12}{}^o}{h^2}) \tag{3}$$

and the unknown functions g_i are given in terms of the crack opening displacements and rotations as follows:

$$g_i(x_2) = \frac{\partial}{\partial x_2}[v_i(+0,x_2) - v_i(-0,x_2)]\ ,\ -a<x_2<a\ ,\ i=1,...,5. \tag{4}$$

After determining the functions g_i the modes I, II and III stress intensity factors along the crack front may be obtained from

$$k_1(x_2) = \sqrt{L}\,(\sigma_1F_1+\sigma_2F_2)\ ,\ k_2(x_2) = \sqrt{L}\,\sigma_3F_3\ ,\ k_3(x_2) = \sqrt{L}\,(\sigma_4F_4+\sigma_5F_5) \tag{5}$$

where the shape functions $F_i(L/h)$ corresponding to a two-dimensional edge crack problem are given in Table 1 and the stresses σ_i are related to g_i through the line spring model and knwon constants c_{ij} by

$$\sigma_i(x_2) = \sum_1^5 c_{ij}\int_{-a}^{x_2} g_j(t)dt\ ,\ -a<x_2<a\ ,\ i = 1,...,5\ . \tag{6}$$

Note that F_i are simply the normalized stress intensity factors for a plate with an edge crack subjected to the external loads defined by (3) (without the superscript o), where $\sigma_{13}=\sigma_3$ is parabolic in x_3 and $\sigma_{13}=\sigma_6$ is a uniformly distributed trnasverse shear stress included in the table for completeness.

3. RESULTS AND DISCUSSION

Even though the line spring model is an approximate method, comparison of the results with the existing three-dimensional finite element solutions indicate that the accuracy of the method is, in fact, quite good. For plates containing semi-elliptic surface cracks under symmetric and antisymmetric loading conditions these comparisons may be found in [1] and [2]. Some sample results showing the mode I stress intensity factors obtained from the line spring model and the finite element calculations [5] for a semielliptic axial surface crack in a pressurized cylindrical shell are given in Fig. 2. The normalizing stress intensity factor K_{ot} shown in the figure is the corresponding two-dimensional edge crack value in a flat plate under membrane loading and is given in Table 1 ($K_{ot}=k_{11}$). Referring to Fig. 1 for notation, in Fig. 2 $y=x_2$ defines the position along the crack front. Note that in Fig. 2 and in all the other examples considered in this study the crack occupies $x_1=0$ plane and $x_1=0$ and $x_2=0$ are assumed to be planes of symmetry or antisymmetry.

Table 1. Shape factors $F_i(L_o/h)$ for a plate with an edge crack of depth L_o under various loading conditions.

$\frac{L_o}{h}$	$F_1 = \frac{k_{11}}{\sigma_1\sqrt{L_o}}$	$F_2 = \frac{k_{12}}{\sigma_2\sqrt{L_o}}$	$F_3 = \frac{k_{23}}{\sigma_3\sqrt{L_o}}$	$F_4 = \frac{k_{34}}{\sigma_4\sqrt{L_o}}$	$F_5 = \frac{k_{35}}{\sigma_5\sqrt{L_o}}$	$F_6 = \frac{k_{26}}{\sigma_6\sqrt{L_o}}$
0	1.1215	1.1215	0	1.0	1.0	1.1215
0.1	1.1892	1.0472	0.2522	1.0041	0.8765	1.1219
0.2	1.3673	1.0553	0.4638	1.0170	0.7594	1.1264
0.3	1.6599	1.1241	0.6392	1.0398	0.6477	1.1419
0.4	2.1114	1.2606	0.7859	1.0753	0.5403	1.1763
0.5	2.8246	1.4972	0.9131	1.1284	0.4368	1.2391
0.6	4.0332	1.9140	1.0339	1.2085	0.3369	1.3450
0.7	6.3549	2.7252	1.1700	1.3360	0.2408	1.5229
0.8	11.955	4.6764	1.3726	1.5650	0.1491	1.8459
0.9	34.632	12.462	1.8368	2.1133	0.0646	2.6037
0.95	99.14	34.306	2.5260	2.9180	0.0273	3.6854

Sample results for toroidal shells with a semi-elliptic surface crack under various loading conditions are shown in Figures 3-7 and Tables 2 and 3. Even though in the examples given the profile of the surface crack is assumed to be semi-elliptic, the method is quite general and can accommodate any prescribed crack profile. Thus, as shown in [1] one may easily track the subcritical propagation of a surface crack once the crack growth model and the load/time history are specified. In figures 3-6 the stress intensity factors are normalized with respect to a constant $\sigma_i\sqrt{h}$ rather than $\sigma_i\sqrt{L_o}$, h and L_o being the shell thickness and the crack depth, respectively. Thus, as $L_o \to 0$ the SIFs approach zero in all cases. Figure 3 shows the variation of the Mode I SIF for a surface crack in a spherical cap as a function of the crack depth L_o and the crack length a. The shell is assumed to be under either membrane loading $\sigma_1=N_{11}/h$ or local bending $\sigma_2=6M_{11}/h^2$, and the crack is semi-elliptic and is located on the outside surface. The effect of the crack location is shown in Fig. 4. From Fig. 4 it may be seen that in a pressurized spherical shell, the SIF for an external crack is somewhat greater than that for the corresponding crack located on the inner surface.

Figure 5 shows the mode I stress intensity factors for a semielliptic crack in a toroidal shell under membrane loading and local bending. In this example the crack is located at position A (see Fig. 1 for notation). From Fig. 5 and Fig. 3 it is seen that in shells under bending SIF becomes negative for sufficiently deep cracks, meaning that for L_o greater than a critical depth the bending solution given would not be valid. In this case the crack faces would close on the compression side and a technique such as that described in [1] must be used to solve the corresponding crack/contact problem. The results shown in Figures 3-5 give the SIF at the mid point of the crack; that is, at $x_2=0$. For various crack locations and loading conditions, some examples showing the distribution of the SIFs along the crack front in a toroidal shell are given in Table 2 where the normalizing SIF, k_{11}, is listed in Table 1. The results given in Table 3 are self-explanatory and show primarily the effect of the elbow curvature,

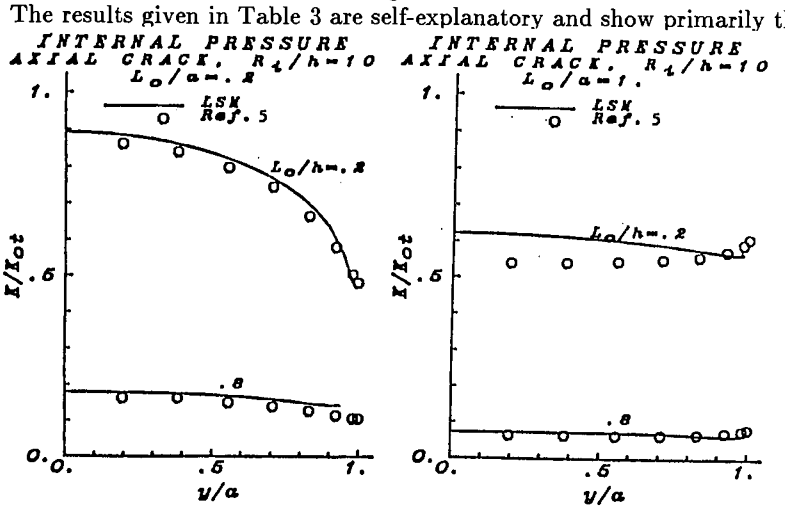

Fig. 2 Comparison of stress intensity factors given by the line spring model and finite element analysis.

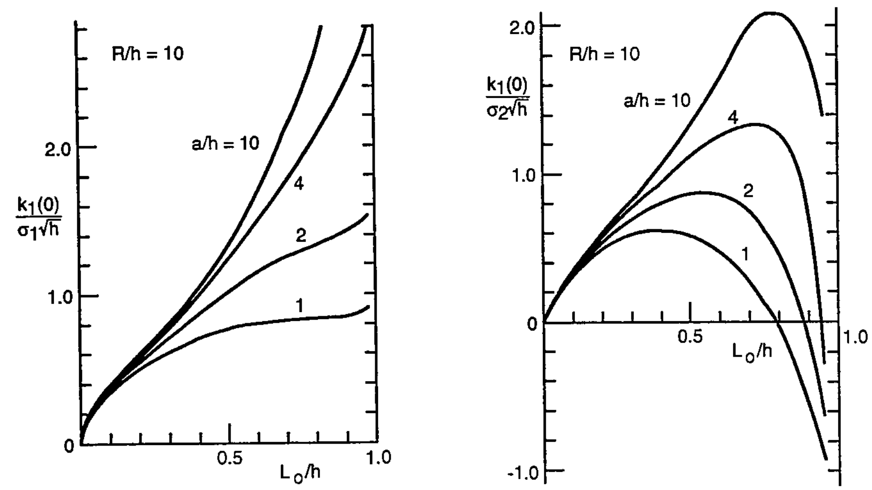

Fig. 3 Mode I SIFs at the center of a semielliptic external surface crack in a spherical shell under membrane loading σ_1 and bending σ_2.

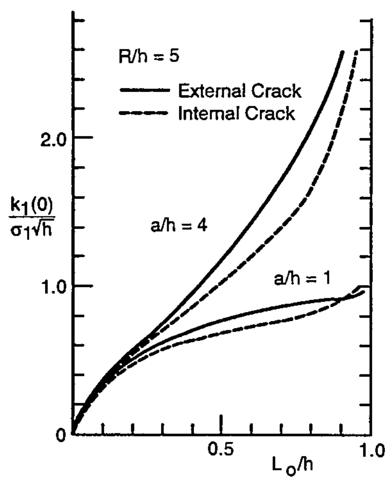

Fig. 4 SIFs for surface cracks in a spherical shell under membrane loading.

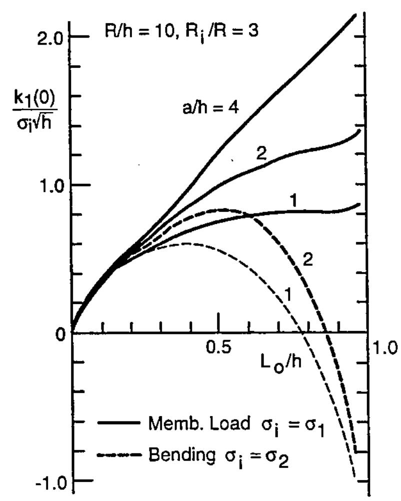

Fig. 5 SIFs for a surface crack in a toroidal shell (crack position A).

crack location and crack depth on the SIFs. One may note that the actual SIFs shown in Figures 3-6 are obtained by multiplying the normalized values given in Tables such as 2 and 3 by $F_i\sqrt{L_o/h}$, where F_i are the shape factors listed in Table 1.

Figure 6 shows the SIF at the midpoint of a semielliptic surface crack at position A in a toroidal shell under inplane shear loading N_{12} (e.g., a pipe elbow under torsion). In this case the stress state along the crack front is primarily mode III. An example for the relative magnitude of the secondary SIF (which is mode II) and the distribution of the SIFs along the crack front in a cylindrical shell are shown in Fig. 7.

Table 2. Normalized stress intensity factors $k_1(x_2)/k_{1i}$, (i=1,2) along a semielliptic surface crack front in a toroidal shell located at various positions (Fig. 1), a/h=1, R/h=10, R_i/R=3, L_o/h=0.4, ν=0.3.

		Internal Crack				External Crack			
	x_2/a	A	B	C	D	A	B	C	D
Membrane Loading	0	0.493	0.497	0.499	0.501	0.512	0.521	0.505	0.512
	0.2	0.489	0.493	0.495	0.497	0.507	0.516	0.501	0.513
	0.4	0.477	0.482	0.483	0.485	0.495	0.503	0.489	0.500
	0.6	0.455	0.460	0.461	0.463	0.471	0.479	0.466	0.477
	0.7	0.439	0.444	0.445	0.447	0.454	0.462	0.450	0.460
	0.8	0.418	0.423	0.423	0.426	0.432	0.439	0.428	0.437
	0.9	0.389	0.394	0.393	0.397	0.401	0.408	0.398	0.406
	0.95	0.367	0.373	0.371	0.375	0.379	0.385	0.376	0.384
	0.98	0.348	0.353	0.352	0.355	0.358	0.364	0.355	0.363
(Local) Bending	0	0.423	0.429	0.431	0.433	0.466	0.457	0.439	0.453
	0.2	0.427	0.433	0.436	0.437	0.449	0.460	0.442	0.456
	0.4	0.438	0.444	0.446	0.448	0.459	0.470	0.453	0.466
	0.6	0.456	0.461	0.462	0.466	0.475	0.485	0.469	0.482
	0.7	0.466	0.472	0.472	0.476	0.484	0.493	0.478	0.490
	0.8	0.476	0.482	0.482	0.486	0.493	0.502	0.488	0.499
	0.9	0.484	0.491	0.490	0.494	0.499	0.507	0.495	0.505
	0.95	0.485	0.492	0.490	0.495	0.499	0.507	0.495	0.505
	0.98	0.481	0.488	0.486	0.491	0.494	0.502	0.491	0.500

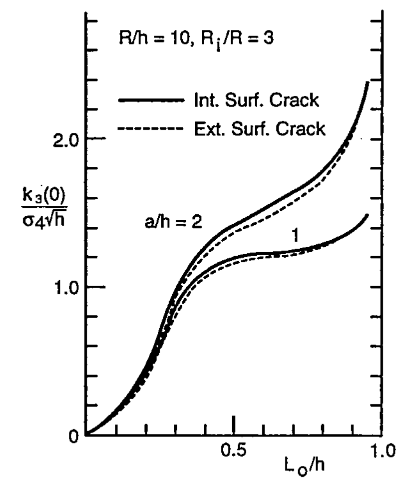

Fig. 6 Mode III SIFs for a surface crack in a toroidal shell under in-plane shear loading N_{12} (crack position A).

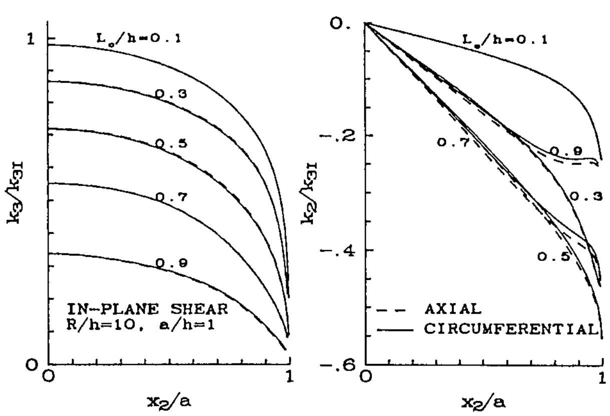

Fig. 7 The variation of SIFs along the crack front for a semi-elliptic external surface crack in a cylindrical shell under in-plane shear loading N_{12}; R/h=10, a/h=1.

Table 3. Normalized stress intensity factor $k_1(0)/k_{11}$ in a toroidal shell with an external semi-elliptic surface crack at various locations; membrane loading, R/h=10, ν=0.3 (Fig. 1).

	R_i/R	a/h=1, L_o/h=					a/h=2, L_o/h=				
		0.2	0.4	0.6	0.8	0.95	0.2	0.4	0.6	0.8	0.95
A	1	.819	.513	.252	.0757	.00866	.883	.633	.351	.115	.0138
	3	.819	.512	.250	.0752	.00861	.882	.630	.348	.113	.0135
	5	.818	.511	.250	.0749	.00859	.881	.629	.346	.112	.0133
	∞	.817	.509	.248	.0743	.00854	.880	.625	.341	.109	.0130
B	1	.823	.520	.257	.0773	.00879	.890	.650	.368	.122	.0145
	3	.824	.520	.257	.0771	.00875	.891	.652	.369	.122	.0143
	5	.824	.520	.256	.0770	.00874	.891	.652	.369	.121	.0142
	∞	.824	.520	.256	.0768	.00871	.892	.653	.369	.121	.0141
C	1	.813	.502	.244	.0744	.00888	.875	.614	.333	.110	.0140
	3	.815	.505	.245	.0739	.00859	.877	.618	.335	.108	.0131
	5	.816	.506	.246	.0739	.00855	.878	.620	.336	.108	.0130
	∞	.817	.509	.248	.0743	.00854	.880	.625	.341	.109	.0130
D	1	.817	.509	.249	.0753	.00880	.879	.623	.342	.112	.0140
	3	.822	.517	.254	.0762	.00871	.889	.645	.361	.118	.0139
	5	.823	.519	.255	.0764	.00870	.890	.650	.365	.119	.0139
	∞	.824	.520	.256	.0768	.00871	.892	.653	.369	.121	.0141
		Internal Surface Crack									
A	1	.807	.492	.237	.0727	.00885	.864	.591	.312	.102	.0136
	3	.808	.493	.237	.0725	.00878	.865	.592	.312	.102	.0133
	5	.808	.493	.238	.0724	.00875	.865	.592	.313	.101	.0132
	∞	.810	.494	.238	.0723	.00867	.867	.594	.313	.101	.0129

REFERENCES

1. Joseph, P.F. and Erdogan, F. (1989), Surface Crack Problems in Plates, Int. Journal of Fracture, **41**, 105-131.
2. Joseph, P.F. and Erdogan, F. (1991), Surface Cracks in a Plate under Antisymmetric Loading Conditions, Int. J. Solids Structures, **27**, 725-750.
3. Delale, F. and Erdogan, F. (1982), Application of the Line-Spring Model to a Cylindrical Shell Containing a Circumferential or Axial Part-Through Crack, ASME Journal of Applied Mechanics, **49**, 97-102.
4. Joseph, P.F. and Erdogan, F. (1990), A Surface Crack in Shells Under Mixed-Mode Loading Conditions, ASME Journal of Applied Mechanics, **55**, 795-804.
5. Raju, I.S. and Newman, Jr., J.C. (1982), Stress Intensity Factors for External and Internal Surface Cracks in Cylindrical Vessels, ASME Journal of Pressure Vessel Technology, **104**, 293-298.